Blind Parallel Interrogation of Ultrasonic Neural Dust Motes Based on Canonical Polyadic Decomposition: a Simulation Study

Alexander Bertrand*, Dongjin Seo†, Jose M. Carmena†‡, Michel M. Maharbiz†, Elad Alon† and Jan M. Rabaey†

*KU Leuven - Dept. Electrical Engineering, Stadius Center for Dynamical Systems, Signal Processing and Data Analytics
† Dept. of Electrical Engineering and Computer Sciences, University of California, Berkeley
‡Helen Wills Neuroscience Institute, University of California, Berkeley

***Abstract*—Neural dust (ND) is a wireless ultrasonic backscatter system for communicating with implanted sensor devices, referred to as ND motes (NDMs). Due to its scalability, ND could allow to chronically record electro-physiological signals in the brain cortex at a micro-scale pitch. The free-floating NDMs are read out by an array of ultrasonic (US) transducers through passive backscattering, by sequentially steering a US beam to the target NDM. In order to perform such beam steering, the NDM positions or the channels between the NDMs and the US transducers have to be estimated, which is a non-trivial task. Furthermore, such a sequential beam steering approach is too slow to sample a dense ND grid with a sufficiently high sampling rate. In this paper, we propose a new ND interrogation scheme which is fast enough to completely sample the entire ND grid, and which does not need any information on the NDM positions or the per-NDM channel characteristics. For each sample time, the US transducers transmit only a few grid-wide US beams to the entire ND grid, in which case the reflected beams will consist of mixtures of multiple NDM signals. We arrange the demodulated backscattered signals in a 3-way tensor, and then use a canonical polyadic decomposition (CPD) to blindly estimate the neural signals from each underlying NDM. Based on a validated simulation model, we demonstrate that this new CPD-based interrogation scheme allows to reconstruct the neural signals from the entire ND grid with a sufficiently high accuracy, even at relatively low SNR regimes.**

I. Introduction

Chronic high-resolution electro-physiological recordings in the brain or the peripheral nervous system would allow for major breakthroughs in the field of neuro-stimulation or brain-machine interfaces, allowing to improve life quality for patients suffering from debilitating neurological disorders [1]. In [2] the 'neural dust' (ND) concept has been introduced, consisting of a wireless ultrasonic backscatter system for communicating with implanted passive sensor devices, referred to as ND motes (NDMs). Very recently, a ND system has been validated in-vivo to record electro-physiological activity in the peripheral nervous system of a rat [3]. Although [3] uses mm-scale NDMs, the ND concept has been shown to be scalable to sub-mm scale, which one day could allow to *chronically* and *wirelessly* record electro-physiological signals within the brain cortex at a micro-scale pitch [2]. To this end, a large number of free-floating NDMs is implanted in the cortex at a 2mm depth in a grid with a 100 μm pitch, in which each NDM measures action potentials or 'spikes' generated by nearby neuron cells [2], [4]. A grid of 'interrogators' equipped with ultrasound (US) transceiver arrays are attached to the cortex to collect the neural signals measured by the NDMs. The NDMs modulate their recorded neural signal onto a reflected US carrier through passive backscattering, which the interrogator then demodulates and at its turn transmits the result through the skull to an external transceiver based on near-field electromagnetic communication [2], [4].

As the system is based on passive backscattering, multiple NDMs will reflect the US carrier, generating major interference when reading out the signal of a targeted NDM. In [4], it was demonstrated that this interference can be suppressed by combining transmit (Tx) and receive (Rx) beamforming techniques to target individual NDMs. However, this technique assumes that the NDM positions or the channel characteristics between the individual NDMs and the US transducers can be estimated, which is a non-trivial task in itself. Furthermore, this approach requires a sequential interrogation of the NDMs based on time-multiplexing, in which the number of Tx-Rx time slots directly depends on the ND grid density. Due to the high sampling rate at which every NDM has to be sampled (typically >20kHz), and since each Tx-Rx time slot should be longer than the time of flight of the US wave, only 10% of a ND grid with 100μm pitch can be read out.

In this paper, we propose a new ND interrogation scheme in which the number of Tx-Rx time slots is independent of the grid density, allowing to read out an *entire* ND grid with 100μm pitch. Furthermore, it does not need any information on the NDM positions or the channels between the US transducers and the NDMs. In this new interrogation scheme, the US transducers transmit only a few (non-focal) Tx beam patterns that cover the entire grid of NDMs. After demodulation, the reflected beams will contain mixtures of the neural signals observed by the different NDMs. We arrange the demodulated backscattered signals in a 3-way tensor, where the dimensions consist of (1) the number of US transducers, (2) the number of collected time samples of the neural signals, and (3) the number of Tx US beam patterns per time sample. We use the canonical polyadic decomposition (CPD) to decompose the tensor in rank-1 terms, and we show that -under certain conditions- each term will only contain the neural signals of a single NDM. This blind CPD-based interrogation scheme allows to read out the entire NDM grid, which is validated on

This work was supported by the KU Leuven Research Council C14/16/057 and Research Project FWO G0D7516N for A.B., the NSF Graduate Fellowship for D.S., and the Bakar Fellowship for J.M.C. and M.M.M.

simulated data using the physical ND model described in [2], [4], which has been experimentally validated in [5] and in [6].

II. Data model

In this section, we briefly review the ND data/simulation model of [2], [4]. Consider a ND system consisting of a linear grid of K NDMs with a 100μm pitch as shown in Fig. 1. A linear array with Q square-shaped 100μm$\times$100μm US transducers (TDs) transmits US carrier waves to the NDM grid over a depth of 2 mm in the neocortex. The carrier signal transmitted by TD q consists of a sinusoid[1] of which the amplitude and phase at time t are represented by the complex-valued signal $X_q(t)$. The corresponding US signal that is observed at time t at the k-th NDM is then given by

$$S_{kq}(t) = H_{kq} \cdot X_q(t) \tag{1}$$

where H_{kq} is a complex-valued channel coefficient that models an attenuation and a phase shift of the US carrier wave, which depends on various factors such as, e.g., the distance between NDM k and TD q, the US path loss constant in brain tissue, the directivity gain of TD$_k$, etc. All these effects are taken into account in our simulation model (details in [2], [4]).

The contributions from each transmitting TD are superimposed at NDM k, resulting in the signal

$$S_k(t) = \sum_q S_{kq}(t) = \mathbf{h}_k^T \mathbf{x}(t) \tag{2}$$

where $\mathbf{h}_k = [H_{k1} \ldots H_{kQ}]^T$ and $\mathbf{x}(t) = [X_1(t) \ldots X_Q(t)]^T$. $S_k(t)$ is modulated by the neural signal $V_k(t)$ that is measured at the k-th NDM and the amplitude-modulated signal $V_k(t) \cdot S_k(t)$ is backscattered to the TD array with an omni-directional reflection pattern. By reciprocity, the Rx backscatter signal from NDM k impinging on the interrogator is then given by

$$\mathbf{r}_k(t) = S_k(t) \cdot V_k(t) \cdot \mathbf{h}_k \tag{3}$$

where $\mathbf{r}_k(t)$ is a Q-dimensional complex-valued vector, of which the q-th element contains the observation at TD q. Based on the superposition principle, the contribution from the entire ND grid on the TD array is

$$\mathbf{r}(t) = \sum_{k=1}^{K} \mathbf{r}_k(t) + \mathbf{n}(t) \tag{4}$$

where $\mathbf{n}(t)$ represents additive channel and receiver noise. Our goal is to extract $V_k(t)$, for all $k = 1, \ldots, K$ based on $\mathbf{r}(t)$.

It is noted that, for the sake of clarity, the above model is a slightly simplified representation of the actual physical model in [2]. Nevertheless, the simulated data on which we will validate our method (see Section IV) is generated using the complete physical model in [2], [4].

III. CPD-based interrogation of neural dust grids

A. Canonical Polyadic Decomposition

The Canonical Polyadic Decomposition (CPD), a.k.a. PARAFAC or CANDECOMP, decomposes a tensor into a sum

[1]In our simulations, the carrier frequency is set to f_c=10MHz, which corresponds to a wavelength of λ = 150 μm in tissue [2].

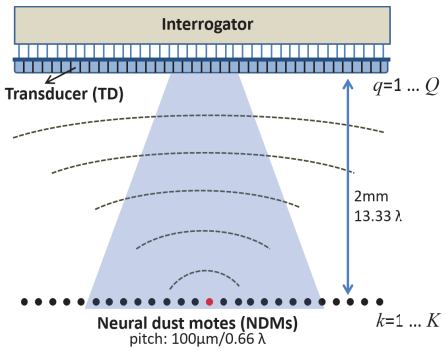

Fig. 1. Schematic representation of the neural dust system.

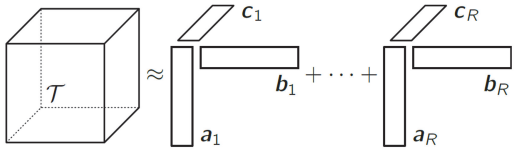

Fig. 2. CPD of a 3-way tensor (figure from Tensor Lab user guide [8]).

of rank-1 tensors. For a 3-way tensor $\mathscr{R} \in \mathbb{C}^{Q \times T \times P}$, the CPD of order K can be written as (see Fig. 2)

$$\mathscr{R} = \sum_{k=1}^{K} \mathbf{a}_k \circ \mathbf{b}_k \circ \mathbf{c}_k + \mathscr{E} \tag{5}$$

where $\mathbf{a}_k$, $\mathbf{b}_k$, and $\mathbf{c}_k$ are Q-, T-, and P-dimensional vectors, respectively, $\circ$ denotes the outer product, and where $\mathscr{E}$ denotes a possible error term in case the tensor rank is larger than K. The least-squares based CPD will try to find $\mathbf{a}_k$, $\mathbf{b}_k$, and $\mathbf{c}_k$ such that the squared entries of $\mathscr{E}$ are minimized.

As opposed to matrix decompositions, tensor decompositions such as the CPD often have milder uniqueness properties, even without imposing any constraints on the factors (such as statistical independence or orthogonality), which makes them very useful for blind source separation.

Definition (Kruskal Rank): The Kruskal rank of a matrix $\mathbf{A}$ is the largest number j such that *any* set of j columns of $\mathbf{A}$ is linearly independent.

Corollary: If all columns of a $Q \times K$ matrix $\mathbf{A}$ with $Q \geq K$ are linearly independent, then its Kruskal rank is equal to K, i.e., the number of columns.

Let $\mathbf{A}$ denote the $Q \times K$ matrix containing all $\mathbf{a}_k$'s in its columns, and let Kr_A denote the Kruskal rank of this matrix (and similarly for the matrices $\mathbf{B}$ and $\mathbf{C}$). Assuming $\mathscr{R}$ can be written as a sum of K rank-1 tensors, then a sufficient condition for the CPD to be unique[2] is that [7]

$$Kr_A + Kr_B + Kr_C \geq 2K + 2\,. \tag{6}$$

It is noted that this is a sufficient condition, and less strict or generic uniqueness conditions have later been proposed [7].

B. A CPD-compatible model of neural dust

We will now construct a tensor based on the backscatter signals from a neural dust grid, which approximately satisfies

[2]Uniqueness is up to an arbitrary non-zero scaling of the 3 factors and a permutation of the K terms.

the CPD model (5) and the uniqueness condition (6). The main idea is to read out each sample of $V_k(t)$ multiple times, but with different ultrasound excitation (i.e., different amplitude and phase). To this end, for each time slot of length ε seconds, the TD array creates a different random Tx beam pattern by letting each of the Q TDs add a random phase to the carrier.

Let us first consider a single NDM, say mote k. Assume that NDM k at time t is excited with a US wave with amplitude $a(t)$ and phase $\phi(t)$, i.e., $S_k(t) = a(t)e^{j\phi(t)}$. At the TD array in Rx mode, this will be observed as (see (3))

$$\mathbf{r}_k(t) = a(t)e^{j\phi(t)} \cdot V_k(t) \cdot \mathbf{h}_k \tag{7}$$

where we ignored the thermal noise[3] in (4). Since the TD array changes the Tx beam pattern after every ε seconds, the same NDM k is excited at time $t+\varepsilon$ with a US wave with different amplitude $a(t+\varepsilon)$ and phase $\phi(t+\varepsilon)$. If we now assume that $1/\varepsilon$ is at least P times larger than the effective bandwidth of $V_k(t)$, then it holds that $V_k(t) \approx V_k(t+n\varepsilon)$, $\forall\, n \in \{1,\ldots,P\}$, and hence

$$\forall\, n \in \{1,\ldots,P\} : \mathbf{r}_k(t+(n-1)\varepsilon) \approx V_k(t) \cdot c_{k,n} \cdot \mathbf{h}_k \tag{8}$$

where

$$c_{k,n} = a(t+(n-1)\varepsilon)e^{j\phi(t+(n-1)\varepsilon)} \,. \tag{9}$$

Define the matrix

$$\mathbf{R}_k(t) = [\mathbf{r}_k(t)\, \mathbf{r}_k(t+\varepsilon) \ldots \mathbf{r}_k(t+(P-1)\cdot\varepsilon)] \,. \tag{10}$$

Then, based on (8), we can observe that $\mathbf{R}_k(t)$ has a rank-1 structure

$$\mathbf{R}_k(t) \approx V_k(t) \cdot \mathbf{h}_k \cdot \mathbf{c}_k^T \tag{11}$$

where $\mathbf{c}_k$ is a P-dimensional vector containing the coefficients $c_{k,n}$ as defined in (9). The vector $\mathbf{c}_k$ in (11) can be considered to be a P-dimensional random complex-valued vector, which will be different for each NDM k due to the different positions of the NDMs and the random Tx phases chosen at the TD array.

Let $f_s = 1/\Delta$ denote the sampling rate at which we aim to read out the neural signal $V_k(t)$ (typically $f_s = 20$kHz). In the sequel, we refer to sample times according to f_s as 'neural samples', and we refer to sample times according to $1/\varepsilon$ as 'Tx/Rx samples'. Assume that P and ε are chosen such that $\Delta = P \cdot \varepsilon$, i.e., the Tx/Rx sampling rate is P times larger than the neural sampling rate, such that (8) holds. For each neural sample time of $V_k(t)$, we then collect P Tx/Rx samples of $\mathbf{r}_k(t)$ at the transducer array, which we use to populate the $Q \times P$ rank-1 matrix $\mathbf{R}_k(t)$, as defined in (10)-(11).

We now assume that the random Tx beam pattern, i.e., the vector $\mathbf{c}_k$, repeats itself after every $P \cdot \varepsilon = \Delta$ seconds, i.e., after every P Tx beams, the transducers repeat the same Tx sequence. A crucial observation is now that, due to the Δ-periodicity of the beam patterns, each matrix $\mathbf{R}_k(t)$ for each neural sampling time $t \in \{0, \Delta, 2\Delta, \ldots\}$ is exactly the same complex-valued rank-1 matrix up to a real-valued amplitude scaling with $V_k(t)$, i.e.,

$$\mathbf{R}_k(t+n\Delta) \approx V_k(t+n\Delta) \cdot \mathbf{h}_k \cdot \mathbf{c}_k^T \,. \tag{12}$$

[3]In section IV, we will investigate the influence of noise.

By collecting all these matrices for different neural sampling times into a tensor $\mathscr{R}_k$, we can easily see that this will be a rank-1 tensor, i.e.,

$$\mathscr{R}_k \approx \mathbf{a}_k \circ \mathbf{b}_k \circ \mathbf{c}_k \tag{13}$$

where

$$\mathbf{a}_k \sim \mathbf{h}_k \tag{14}$$

$$\mathbf{b}_k \sim [V_k(0)\, V_k(\Delta)\, V_k(2\Delta) \ldots]^T \tag{15}$$

$$\mathbf{c}_k \sim [c_{k,1}\, c_{k,2} \ldots c_{k,P}]^T \,. \tag{16}$$

If we now consider all K NDMs, we can use the superposition principle to see that the tensor based on the superimposed Rx waves is equal to

$$\mathscr{R} = \sum_{k=1}^{K} \mathscr{R}_k \approx \sum_{k=1}^{K} \mathbf{a}_k \circ \mathbf{b}_k \circ \mathbf{c}_k \tag{17}$$

and hence it satisfies the CPD model (5). The CPD (17) can be computed using the free Matlab toolbox 'Tensor Lab' [8].

Note that the number of Tx-Rx time slots (per second) to populate $\mathscr{R}$ is $P \cdot f_s$, which is independent of the number of NDMs K. This is different from the original approach where each NDM is read out sequentially, in which case the number of Tx-Rx time slots is directly depending on K.

C. Uniqueness of the neural dust CPD

If we can guarantee that the CPD of the complex-valued tensor $\mathscr{R}$ obtained in (17) is unique, then we know that the factors $\mathbf{b}_k$ will contain the samples of the individual neural signals $V_k(t)$, $\forall\, k \in \{1,...,K\}$ (up to an arbitrary complex-valued scaling for each k, see Subsection III-D). As a by-product, we find the channel coefficients $\mathbf{h}_k$ in the factors $\mathbf{a}_k$.

Note that the number of components in the CPD is equal to the number of NDMs K. This means that the matrices $\mathbf{A}$, $\mathbf{B}$, and $\mathbf{C}$ have dimensions $Q \times K$, $T \times K$, and $P \times K$, respectively, where T is the number of collected neural samples. The entries in the matrix $\mathbf{A}$ correspond to channel coefficients, the entries in $\mathbf{B}$ correspond to neural signal samples, and the entries in $\mathbf{C}$ correspond to the local observation of P different beam patterns at the NDMs. The entries in these matrices can be viewed as random complex numbers where each individual column depends on the *position* of the corresponding NDM (for $\mathbf{A}$ and $\mathbf{C}$) or the *samples* of the neural signals (for $\mathbf{B}$). Because these positions and samples are different for each NDM, we can assume that $\mathbf{A}$ and $\mathbf{B}$ will have K linearly independent columns, and $\mathbf{C}$ will have P independent rows, so all three matrices will have full rank with high probability.

If we assume that $Q \geq K$ (sufficient TDs), and $T \geq K$ (sufficiently long sample window), then both $\mathbf{A}$ and $\mathbf{B}$ will be tall matrices, and hence we can assume based on the corollary in Subsection III-A that $Kr_A = Kr_B = K$ with probability 1. As the sum of the Kruskal ranks of $\mathbf{A}$, $\mathbf{B}$, and $\mathbf{C}$ must be larger than $2K+2$, we eventually obtain the condition that $Kr_C \geq 2$, i.e., any 2 out of K columns of the $P \times K$ matrix $\mathbf{C}$ must be linearly dependent. In principle this holds if $P \geq 2$ (with probability 1) due to the randomness of the entries in

C. Nevertheless, if K is large, and if $P = 2$, there is a high probability that there exist 2 out of K random 2-D vectors that are *approximately* the same. This will make the CPD ill-conditioned, and the decomposition will give inaccurate source separation results. Therefore, P should be chosen as large as possible. Indeed, in a higher dimensional space, the probability of observing two (out of K) random points that are close to each other quickly decreases. However, note that the value of P will be bounded by the number of different US beam patterns that can be transmitted, reflected, received, and demodulated within one interval of Δ seconds. Based on these constraints and using the ND model in [2], P can not be chosen larger than 10 for a neural sampling rate of 20kHz (details omitted).

D. Extracting real-valued neural samples from complex-valued CPD factors

The CPD is only unique up to an arbitrary scaling of the 3 factors ($\mathbf{a}_k$, $\mathbf{b}_k$, $\mathbf{c}_k$) in each component k. This is a fundamental ambiguity in any blind source separation problem, which is usually not a issue if only the shape of the source signal is of interest, rather than its true amplitude. However, in our case this arbitrary scaling is complex-valued, whereas the signal $V_k(t)$ is a real signal. Therefore, we have to find an amplitude-preserving complex scaling factor that makes the imaginary part of all entries in $\mathbf{b}_k$ as small as possible, i.e., our goal is to find a rotation in the complex plane such that $\Im(\mathbf{b}_k) \approx 0$. Let $\mathbf{B}_k$ be a 2-column matrix that contains the real and imaginary part of $\mathbf{b}_k$ in its two columns, i.e.,

$$\mathbf{B}_k = [\Re(\mathbf{b}_k)\, \Im(\mathbf{b}_k)]\,. \tag{18}$$

Then we aim to find an orthogonal (rotation) matrix $\mathbf{Q}$ such that the entries in the second column of

$$\tilde{\mathbf{B}}_k = \mathbf{B}_k \mathbf{Q} \tag{19}$$

are as close to zero as possible. In theory, the second column can be made exactly zero, since all rows of $\mathbf{B}_k$ should be collinear as $\mathbf{b}_k$ consists of real-valued samples of $V_k(t)$, which are all multiplied by the same (unknown) complex-valued scalar. However due to noise and model deviations, this will only be approximately satisfied. Finding the optimal rotation boils down to a principal component analysis, which can be solved using the singular value decomposition of $\mathbf{B}$:

$$\mathbf{B}_k = \mathbf{U}\Sigma\mathbf{Q}^T \tag{20}$$

from which we obtain the orthogonal 2×2 matrix $\mathbf{Q}$. The first column of Q will project the rows of $\mathbf{B}_k$ onto the first principal component, hence the first column of $\tilde{\mathbf{B}}_k$ contains an estimate of the samples of $V_k(t)$ (up to a real-valued scaling and sign ambiguity), which we denote as $\tilde{V}_k(t)$.

IV. Simulation Results

A. Performance Metric

As a performance metric, we use the signal-to-error ratio (SER), which quantifies the total error power between the reconstructed $\tilde{V}_k(t)$ and the true neural signal $V_k(t)$, relative to the power of $V_k(t)$ (a high SER is better), i.e.,

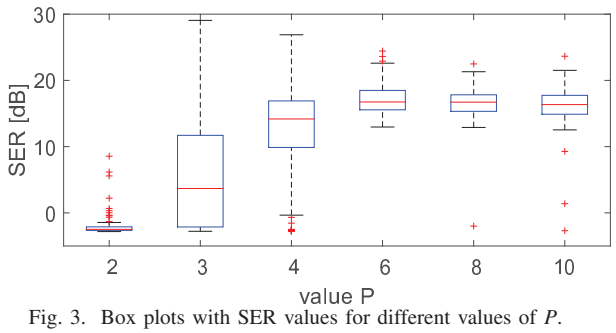

Fig. 3. Box plots with SER values for different values of P.

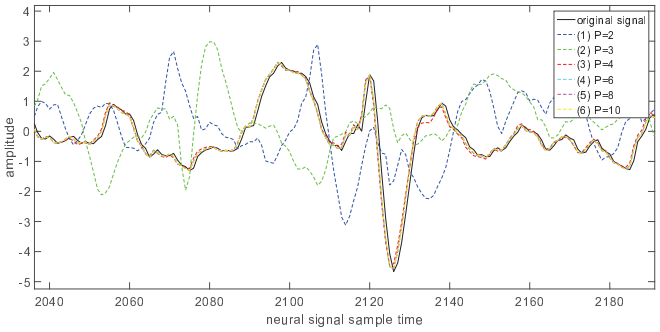

Fig. 4. Reconstruction of $V_k(t)$ for different values of P (for $k = 67$, i.e., a NDM in the middle of the grid)

$$SER_k = \max_{\alpha \in \mathbb{R}} 10 \cdot \log_{10} \frac{\sum_t V_k(t)^2}{\sum_t (V_k(t) - \alpha \tilde{V}_k(t))^2} \tag{21}$$

where α is used to resolve the scaling ambiguity in $\tilde{V}_k(t)$.

B. Simulation results

The simulation data is generated using the physical model described in [2], [4]. We show simulation results for a 1D-grid of $K = 133$ NDMs, and an array of $Q = 180$ TDs. The center point distance between the NDMs is 150 μm, whereas this is 100 μm for the interrogator transducer array elements (resulting in $Q > K$). The signals $V_k(t)$ are mutually uncorrelated and consist of synthetic action potential signals, i.e., neural spikes, with superimposed biological noise (details in [4]). Unless stated otherwise, we computed the CPD of order $K = 133$, i.e., with exactly as many components as there are NDMs. We use 10000 neural samples which corresponds to a 0.5s segment of the signal $V_k(t)$ ($f_s = 20$kHz), resulting in a tensor of dimension $180 \times 10000 \times P$.

In Fig. 3, we demonstrate how the SER improves as a function of P. The boxplots capture the SER values over all $K = 133$ NDM signals (red points indicate outliers). We find that P should satisfy $P \geq 4$ in order to have a decent performance (although a significant number of NDMs is still poorly reconstructed if $P = 4$).

In Fig. 4, we show a time segment of the original signal $V_k(t)$, and the reconstructed signal by using the CPD (for different values of P). This shows that the CPD is able to accurately demix the different NDM signals if $P \geq 4$. Note that the CPD can introduce a delay ambiguity of one sample. This is because the derivation of our CPD model assumes that every P

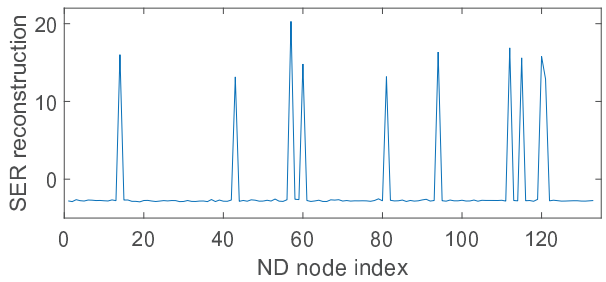

Fig. 5. SER for each NDM signal when using a CPD of order 10, whereas $K = 133$ (with $P = 8$).

subsequent Tx/Rx samples $[V_k(t)\,V_k(t+\varepsilon)\,\ldots\,V_k(t+(P-1)\varepsilon)]$ correspond to the same neural sample, i.e., either $V_k(t)$ or $V_k(t+\Delta) = V_k(t+P\varepsilon)$, yielding a 1-sample ambiguity.

In Fig. 5, we investigate how a low-order CPD performs, i.e., whether it keeps its demixing ability if the number of NDMs is underestimated and hence a CPD is computed with less components than the true number of underlying NDMs. To this end, we have computed a CPD with only 10 components (with $P = 8$). As demonstrated in Fig. 5, the 10 extracted components indeed correspond to 10 NDM signals with a decent reconstruction quality (SER>10dB), and hence the remaining 123 NDM signals are not mixed in these 10 components. Of course, we do not know *which* NDM signals are extracted. However, we can use the steering vector estimates in the matrix $\mathbf{A}_k$ to identify the position of the NDMs corresponding to the extracted signals.

Finally, we have performed a down-scaled experiment, in which only 10 neighboring TD elements are activated in Tx (with $P = 8$), and where 30 TDs (the 10 Tx TDs + 2×10 neighboring TDs on both sides) are activated in Rx. This results in a tensor with dimension $30 \times 10000 \times 8$. As the number of Rx TDs (30) is much smaller than the total number of NDMs ($K = 133$), we can only extract a subset of the neural signals. Furthermore, since only 10 TDs are active in Tx mode, only a region with approximately 30 NDMs will reflect a significant amount of US energy. We compute a CPD of order 15 (i.e., 15 components). The reconstruction accuracy for all NDMs is shown in Fig. 6. It is observed that the 15 NDM signals that are accurately extracted (SER> 10 dB) come from adjacent NDMs. These are the NDMs that are closest to the Tx TDs, as these capture and reflect the most energy.

In Fig. 7, we plot the result of the previous experiment for different levels of Rx thermal noise $\mathbf{n}(t)$ in (4). We find that the CPD-based extraction method is quite robust to noise, even in low-SNR scenarios (up to 0dB). An SNR of 0dB means that the noise power at one transducer element is equal to the power of the superimposed reflected ultrasound waves observed at a single transducer element. We still get reasonably high SER values for such noisy conditions, which means that the CPD also has noise reduction capabilities. Indeed, since spatio-temporally white noise does not have a low-rank structure in the tensor, the CPD can not model it well and hence most of the noise power will be shifted to the error term in (5).

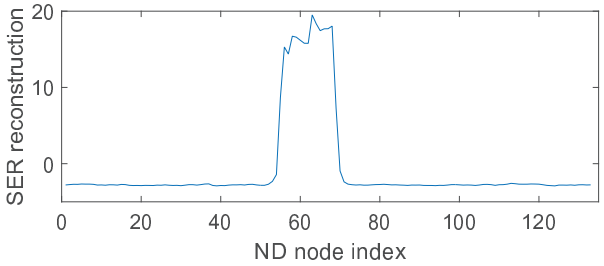

Fig. 6. SER for each NDM signal when using only 10 TDs for Tx, and 30 TDs for Rx using a CPD of order 15 (with $P = 8$).

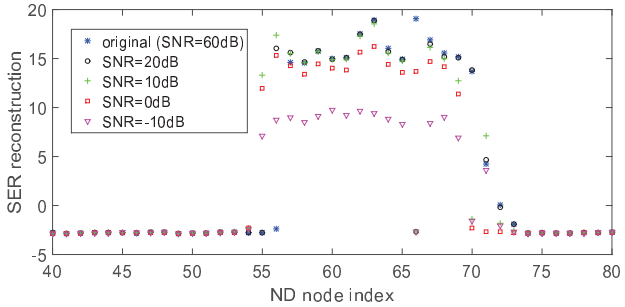

Fig. 7. SER for 15 reconstructed NDMs for different levels of Rx noise.

V. Conclusions

We have presented a new CPD-based interrogation scheme for ND, which allows to interrogate a dense grid of NDMs. As opposed to previous approaches, we do not need to know the channel or position of the NDMs, and we can read out the entire grid, rather than just a subset. Based on a simulation study, the proposed method obtains a good reconstruction accuracy.

References

[1] J. Collinger *et al.*, "High-performance neuroprosthetic control by an individual with tetraplegia," *The Lancet*, no. 9866, pp. 557–564, 2013.

[2] D. Seo, J. Carmena, J. Rabaey, E. Alon, and M. Maharbiz, "Neural dust: An ultrasonic, low power solution for chronic brain- machine interfaces," *arXiv:1307.2196*, Jul. 2013.

[3] D. Seo, R. M. Neely, K. Shen, U. Singhal, E. Alon, J. M. Rabaey, J. M. Carmena, and M. M. Maharbiz, "Wireless recording in the peripheral nervous system with ultrasonic neural dust," *Neuron*, vol. 91, no. 3, pp. 529 – 539, 2016.

[4] A. Bertrand, D. Seo, F. Maksimovic, J. M. Carmena, M. M. Maharbiz, E. Alon, and J. M. Rabaey, "Beamforming approaches for untethered, ultrasonic neural dust motes for cortical recording: a simulation study," in *Proc. Int. Conf. of the IEEE Engineering in Medicine and Biology Society (EMBC)*, Chicago, Illinois, USA, 2014.

[5] D. Seo, J. M. Carmena, J. M. Rabaey, M. M. Maharbiz, and E. Alon, "Model validation of untethered, ultrasonic neural dust motes for cortical recording," *Journal of Neuroscience Methods*, vol. 244, pp. 114 – 122, 2015, brain Computer Interfaces; Tribute to Greg A. Gerhardt.

[6] D. Seo, H. Y. Tang, J. M. Carmena, J. M. Rabaey, E. Alon, B. E. Boser, and M. M. Maharbiz, "Ultrasonic beamforming system for interrogating multiple implantable sensors," in *2015 37th Annual International Conference of the IEEE Engineering in Medicine and Biology Society (EMBC)*, Aug 2015, pp. 2673–2676.

[7] I. Domanov and L. De Lathauwer, "On the uniqueness of the canonical polyadic decomposition of third-order tensors - part i: Basic results and uniqueness of one factor matrix," *SIAM Journal on Matrix Analysis and Applications (SIMAX)*, vol. 34, no. 3, pp. 855–875, 2013.

[8] L. Sorber, M. Van Barel, and L. De Lathauwer, "Tensorlab v2.0," 2014. [Online]. Available: http://www.tensorlab.net